

# An assessment of the usefulness of handheld X-ray devices in general radiography based on a performance evaluation experiment

E. Kim, H. Park, H. Choi, J. Kim\*

Department of Health and Safety Convergence Science, Korea University, Seoul, Republic of Korea

## ABSTRACT

### ► Original article

#### \*Corresponding author:

Dr. Jungmin Kim

E-mail: minbogun@korea.ac.kr

Received: December 2021

Final revised: August 2022

Accepted: August 2022

Int. J. Radiat. Res., July 2023;  
21(3): 545-551

DOI: 10.52547/ijrr.21.3.26

**Keywords:** Handheld X-ray device, portable X-ray device, performance evaluation, image quality, scatter radiation dose.

**Background:** Light and portable handheld X-ray devices are being used more often for diagnosis because they allow radiography procedures to be performed on patients in settings where there may not be stationary X-ray devices, such as islands or mountainous regions. In this study, the performances of handheld X-ray devices (HxD) and stationary X-ray devices (SxD) were compared to determine whether the handheld device could produce diagnostically acceptable image quality outside of hospitals, particularly during a global pandemic. **Materials and Methods:** For performance evaluation, the accuracy of tube voltage, reproducibility of X-ray dose, linearity, leakage dose, and accuracy of focal spot size were obtained. The accuracy of the tube voltage and the reproducibility and linearity of the X-ray dose were measured to reduce the frequency of patient reimaging as a performance evaluation of the devices. **Results:** After conducting various experiments, it was found that the percentage average error (PAE) value of the tube voltage was -0.01% for the HxD, and the error of the tube voltage was 0.01% for the SxD, which is lower than the standard 10%. Additionally, when using an HxD according to these standards, medical staff is considered safe from exposure to leakage dose because the leakage dose is 0.26 mSv/year without the use of a partition. **Conclusion:** Our results provide evidence that images of appropriate quality can be taken with an HxD, offering comparable diagnostic value. It was concluded that the leakage radiation dose would be safe at 0.26 mSv/year without using a radiation shielding partition.

## INTRODUCTION

Because of the COVID-19 pandemic, the number of hospitalized patients worldwide has increased to the extent that hospitals are saturated, and the frequency of radiography procedures has increased accordingly. To judge the recovery process of patients infected with SARS-CoV-2, chest computed tomography (CT) and general chest radiography are being actively performed <sup>(1)</sup>. Various problems can be encountered in the process of transporting a patient to the radiology department. Complications related to transportation occur in more than 70% of critically ill patients, and the risk of cardiopulmonary arrest has been found to greatly increase when patients' ventilators are replaced with portable ones <sup>(2-6)</sup>.

Additionally, in the process of transporting an infected patient from the isolation ward or negative pressure ward to the radiology room, transmission of the virus to surrounding healthcare providers, related workers, patients, and their family members can increase <sup>(4,7)</sup>. The usefulness of radiation devices that can be transported to patient rooms and perform radiography procedures there has been highlighted in various studies <sup>(2, 8-11)</sup>. Chest radiography in a patient's room using a portable radiation device is

the most commonly performed examination today <sup>(12-15)</sup>. The Republic of Korea has excellent access to medical care, and because of the influence of medical insurance and medical expense insurance, and the rapid aging of the population, the number of uses of diagnostic radiography rapidly increased from 312 million in 2016 to 370 million in 2019 <sup>(16)</sup>. In addition to this trend, from 2016 to 2018, the number of diagnostic radiation generators increased from 22,191 to 26,642 and the number of computed tomography procedures increased from 9,454 to 12,805. As of 2018, a total of 88,294 diagnostic radiation generators were installed and operated in the Republic of Korea <sup>(17)</sup>. As the demand for radiographic examinations increases, it is necessary to promote the use of portable radiation devices that not only reduce the burden on hospitals, other medical facilities, and healthcare providers, but also minimize the transportation of patients with life-threatening conditions.

In the last 20 years, digital-based radiation detectors have replaced screen-film detectors, and post-processing functions paired with image acquisition devices have made high-quality images possible while reducing radiation dosages <sup>(15, 18-20)</sup>. Digital-based detectors reconstruct low-dose images

using post-processing functions and store them in a picture archiving and communication system so that the images can be viewed anytime, anywhere, and by anybody who has access (20-22). Through this image acquisition and sharing process, various efforts are being made to reduce the risk of re-exposure to patients and the overall radiation dose exposure. Owing to this trend in medical diagnostic procedures, clinical trials using handheld X-ray devices (HXDs) and digital-based detectors for chest imaging are increasing.

After the Kevex X-Ray Corporation first developed military use of HXDs in the United States in 1993, nearly 95% of HXDs were used for dental radiography (23). By expanding the use of HXDs, radiologic technologists can take radiographs in various places without the need for patient movement, and it is believed that not only can the critical risk to patients from movement be minimized, but also that various benefits can be provided to the many people who cannot access medical facilities. These devices are light, have good battery durability, are compatible with various detectors, and are expected to replace stationary X-ray devices (SXD), which are often greater in volume. Based on these advantages, HXDs are used in screening clinics, island healthcare systems, local public health centers, emergencies where it is difficult to install SXDs, and radiation protection facilities. Without the need to transport patients suspected of being COVID-19-positive to hospitals, diagnostic images can be acquired using an HXD and a portable radiation shielding partition. Therefore, this study assessed the safety and usefulness of HXDs by comparing the performance of one type of HXD with that of an SXD based on the International Electrotechnical Commission (IEC) 60601 standard and image quality through phantom imaging.

## MATERIALS AND METHODS

### Experimental materials

For comparison of device performance, both HXD (Mine 2.7, HDT, Republic of Korea) and SXD (GXR-40S, DRGEM, Republic of Korea) were irradiated under the same conditions (figure 1).

The equipment used for performance evaluation was a multifunction meter (RMI 240A, Gammex, USA) to measure the tube voltage, an ion chamber (2026C, Radcal Corporation, USA) to measure the first radiation, a survey meter (451P-RYP, Fluke Biomedical, USA) to measure the secondary radiation, and a star test pattern (07-509-2, Cardinal Health, USA) to measure the focal spot size. To evaluate the quality of the acquired images and simulate patient imaging, an opaque chest phantom (76-683, Cardinal Health, USA), an opaque skull phantom (76-618, Cardinal Health, USA), a transparent knee phantom (76-075, Cardinal Health, USA), a transparent elbow phantom

(76-067, Cardinal Health, USA), and a transparent hand phantom (76-018, Cardinal Health, USA) were used.

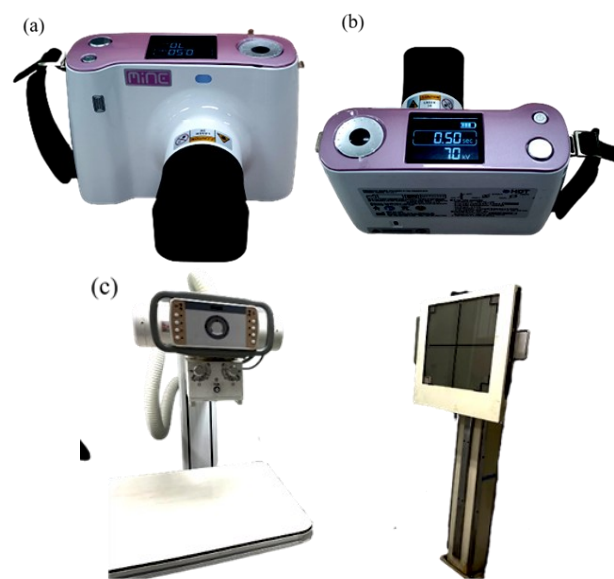


**Figure 1.** X-ray devices used in the experiment (a) handheld X-ray device front view, (b) handheld X-ray device upper view, (c) stationary X-ray device.

For the HXD, the tube voltage was fixed at 70 kVp (kilovoltage peak), the tube current was 2 mA (milliamperes), and the focal spot size was 0.4 mm. When acquiring an image, the exposure time of HXD can be adjusted from 0.01–1.30 seconds. The source-to-image distance can also be adjusted by setting an appropriate length based on the body part being radiographed. The detector that was used with the HXD was a digital-based detector composed of a CsI/GOS scintillator using an a-Si TFT-type sensor. The pixel size was  $3072 \times 3072 \text{ mm}^2$  and the pixel pitch was  $140 \text{ }\mu\text{m}$ . The detector measured  $460 \times 460 \times 15 \text{ mm}^3$  and 3.5 kg, including the battery. When using an HXD, radiographs can be produced by pressing an exposure button. There is also a remote control that can minimize exposure to radiation workers and allow HXDs to be operated from a distance of 2 m or more. In settings where there may be no SXDs installed, such as a screening clinic, an island, or a public health center in a provincial area, the combination of a detector stand for the digital radiography detector and a tripod for the HXD can be used to perform radiography procedures; this experiment was conducted according to these conditions (figure 2).

For the SXD, the tube voltage was adjusted to 40–125 kVp, the tube current was 10–500 mA, and the exposure time was 0.001–10 s. For comparison, the tube voltage of both the HXD and the SXD was set to 70 kVp and the product of tube current radiation time to 2 mAs (milliamperes seconds). The detector used with the SXD was a computed radiography detector with a maximum resolution of  $4020 \times 4892$  and a pixel pitch of  $175 \text{ }\mu\text{m}$ . The detector measured

350 × 450 × 15 mm and 1.5 kg.



**Figure 2.** A detector stands capable of holding the detector and a tripod capable of holding the handheld X-ray device.

#### Tube voltage accuracy test

Radiation exposure from an X-ray device depends primarily on the X-ray tube voltage (kVp), tube current (mA), and exposure time (sec) <sup>(24)</sup>. Thus, it is important to check these parameters to confirm the accuracy of device performance <sup>(25)</sup>. First, to measure the accuracy of the tube voltage of the two devices, the product of the tube voltage and tube current irradiation time was set to 70 kVp and 2 mAs, respectively. A multifunction meter was used for the measurement, and the source-to-image distance was fixed at 40 cm. The percentage average error (PAE) was calculated using equation 1 for the measured results after conducting three investigations.

$$PAE = \frac{x_p - \bar{x}}{\bar{x}} \times 100 (\%) \quad (1)$$

Where;  $x_p$  is the set value, and  $\bar{x}$  is the average value of the measured values.

#### X-ray reproducibility and linearity test

In addition to measuring the accuracy of the radiation voltage, it is important to check the reproducibility and linearity of the radiation dose to confirm the accuracy of device performance <sup>(25)</sup>. To measure the reproducibility and linearity of the radiation dose, the tube voltage of the two devices was fixed at 70 kV, and the tube current–exposure time product was measured at 0.5, 1, and 2 mAs to measure the appropriate radiation dose. An ion chamber was used for the measurements, and the source-to-image distance was fixed at 100 cm. The reproducibility of the radiation dose was evaluated by deriving the coefficient of variation (CV), as shown in equation 2, for the measured results by irradiating

three times for each mAs condition. In addition, the linearity of the radiation dose was evaluated by calculating the radiation dose per mAs for the radiation dose measured under each mAs condition, and by deriving the linearity coefficient, as shown in equation 3.

$$CV = \frac{s}{\bar{x}} = \frac{1}{\bar{x}} \left[ \frac{\sum_{i=1}^n (x_i - \bar{x})^2}{n-1} \right]^{\frac{1}{2}} \quad (2)$$

$$\text{Linearity Coefficient} = \frac{|\text{comparative value (mR/mAs)} - \text{standard value (mR/mAs)}|}{\text{comparative value (mR/mAs)} + \text{standard value (mR/mAs)}} \quad (3)$$

In equation 2,  $s$  is the standard deviation of the measured dose,  $\bar{x}$  is the average of the measured values,  $x_i$  is the measured value of the  $i^{\text{th}}$  dose, and  $n$  is the number of measurements.

#### Leakage dose measurement test

The leakage dose depends on the type of radiation device, the distance from it, and the size of the exposure field. However, according to the 2006 National Academy of Sciences Biologic Effects of Ionizing Radiation Committee report, even a small leakage dose can affect patients or medical staff <sup>(26-27)</sup>. Because of the nature of HXD, radiologic technologists and other operators are likely to be physically close together. Therefore, it is important to measure the leakage dose of radiation devices. To measure the leakage dose of the HXD, radiation was delivered with a tube voltage of 70 kVp and tube current–exposure time product of 1 mA. A survey meter was used for measurements, and measurements were performed three times each in the up, down, left, right, front, and rear directions of the HXD. To increase the measurement sensitivity, the distance between the focus and radiation device was fixed at 10 cm. Regarding the front direction of the HXD, a lead plate with dimensions of 5 × 5 cm<sup>2</sup> and 3 mm was placed in front of the collimator of the device to shield the primary radiation and measure the secondary radiation.

#### Focal spot size accuracy test

The effective focal spot size varies depending on the tube operating conditions; however, the error rate of the device must be within 50% to be recognized as capable of radiography imaging <sup>(28)</sup>. To measure the focal spot size, the tube voltages of both the HXD and SXD were fixed at 70 kV, and the tube current–exposure time products were fixed at 0.5 mAs. The star test pattern was used for measurement, and the distance between the focus and the star test pattern was fixed at 40 cm. The focus and the image receptor, which is the source-to-image distance, were fixed at 80 cm to calculate the focal spot size by doubling the magnification of the image. The distance from the center of the star test pattern image taken from each device to the blurred part of the pattern in the four directions was measured, as shown in figure 3. Subsequently, the focal spot size was derived by substituting the measured length into



equation 4.

$$F = \frac{N}{57.3} \times \frac{D}{(M-1)} \quad (4)$$

Where; N is the angle of the pattern, D is the measurement distance of the image, and M is the magnification used to obtain the focal spot size F.

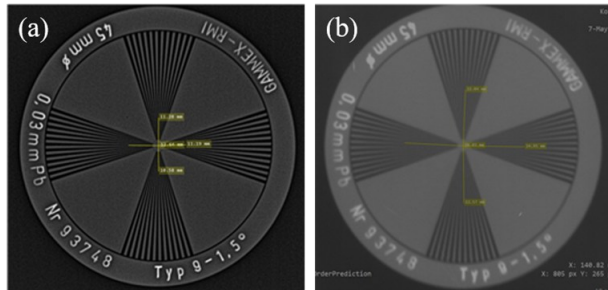


**Figure 3.** Experimental result of star test pattern of (a) handheld X-ray device (b) stationary X-ray device.

### Phantom radiograph test

Phantoms were used to facilitate comparative analysis (29). To evaluate the image quality and simulate patient imaging, five types of phantoms were used. To acquire the posterior-anterior/ anterior-posterior (PA/AP) images, both the HXD and SXD were radiated with a tube voltage of 70 kVp, a tube current–exposure time product of 1 mAs, and a source-to-image distance of 150 cm in combination with an opaque chest phantom for the human body model. To acquire the skull AP image, an opaque skull phantom was used as the human body model. Both the HXD and SXD were radiated with a tube voltage of 70 kVp, a tube current–exposure time product of 1 mAs, and a source-to-image distance of 100 cm. To acquire the knee AP and elbow AP images, a transparent knee phantom and a transparent elbow phantom were used as the human body models. Both devices were radiated with a tube voltage of 70 kVp, a tube current–exposure time product of 0.4 mAs, and a source-to-image distance of 100 cm. Finally, to acquire hand PA images, a transparent hand phantom was used as the human body model. Both devices were radiated with a tube voltage of 70 kVp, a tube current–exposure time product of 0.2 mAs, and a source-to-image distance of 100 cm.

## RESULTS

### Tube voltage accuracy test

HXD had tube voltages of 71, 70.7, and 70.7 kVp, with an average of 70.8. SXD had tube voltages of 69.6, 69.6, and 69.9 kVp, with an average of 69.9. The PAE values for HXD and SXD were -0.01% and 0.01%, respectively.

### X-ray reproducibility and linearity test

The measured radiation doses and CVs of each device are listed in Table 1. HXD showed a CV minimum of 0.001 and a maximum of 0.003, while

SXD showed a CV minimum of 0.005 and a maximum of 0.050. In this experiment, both HXD and SXD had a CV of 0.05 or less, indicating reliable device performance.

The radiation doses and linearity coefficients per milliamperere for each device were calculated using equation 3 and are listed in table 1. The mAs linearity coefficient for HXD was 0.01 when 0.5 mAs was compared with 1 mAs, 0.01 when 0.5 mAs was compared with 2 mAs, and 0.00 when 1 mAs was compared with 2 mAs. The average linearity coefficient was 0.01. In the case of SXD, the linearity coefficients were 0.02, 0.02, and 0.05 in the same order of comparison as that of HXD, and the average linearity coefficient was 0.03.

**Table 1.** Reproducibility and linearity of the handheld X-ray device and the stationary X-ray device.

	Handheld X-ray device (HXD)			Stationary X-ray device (SXD)		
	0.5 mAs	1 mAs	2 mAs	0.5 mAs	1 mAs	2 mAs
Radiation dose (mR)	2.66	2.66	2.66	2.66	2.66	2.66
	5.36	5.36	5.36	5.36	5.36	5.36
	10.78	10.78	10.78	10.78	10.78	10.78
Average Measurement	2.45	2.45	2.45	2.45	2.45	2.45
Coefficient Variant (CV)	0.003	0.002	0.001	0.005	0.050	0.027
Radiation dose per mAs (mR/mAs)	5.30	5.37	5.40	4.91	5.16	5.42
Average Linearity	0.01	0.03	0.00	0.02	0.02	0.05

### Leakage dose measurement test

The average of the leakage dose values measured by location was 0.03  $\mu$ Sv for the upper half, 0.02  $\mu$ Sv for the lower half, 0.10  $\mu$ Sv for the left, 0.09  $\mu$ Sv for the right, 0.02  $\mu$ Sv for the front, and 0.02  $\mu$ Sv for the rear. The left (0.10  $\mu$ Sv) and right (0.09  $\mu$ Sv) sides of the radiation device had the highest values, and the other sides measured between 0.02–0.03  $\mu$ Sv (figure 4).

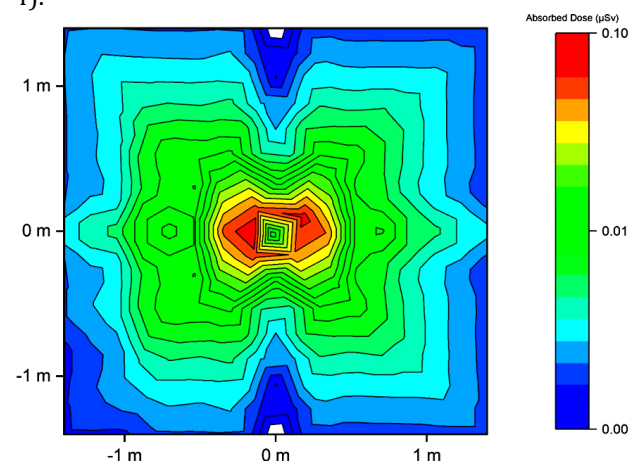


**Figure 4.** Distribution of scatter radiation exposed by handheld X-ray device.

### Focal size accuracy test

The focal spot size of the HXD was 0.62 mm in the direction of the long axis of the X-ray tube and 0.57 mm in the direction perpendicular to the long axis of

the X-ray tube. The focal spot size of the SXD was 1.28 mm in the direction of the long axis of the X-ray tube and 1.17 mm in the direction perpendicular to the long axis.

### Phantom radiograph test

The chest PA/AP radiographic images taken from each device are shown in Figure 5 (a, b). In addition, the original radiation conditions of the SXD, which were 120 kVp, 4 mAs, and source-to-image distance of 180 cm, were used to compare the results of chest radiography (figure 5 [c]). The results from the skull AP image (a-1, b-1), knee AP and elbow AP images (a-2, a-3, b-2, b-3), and hand PA images are shown in figure 6 (a-4, b-4).

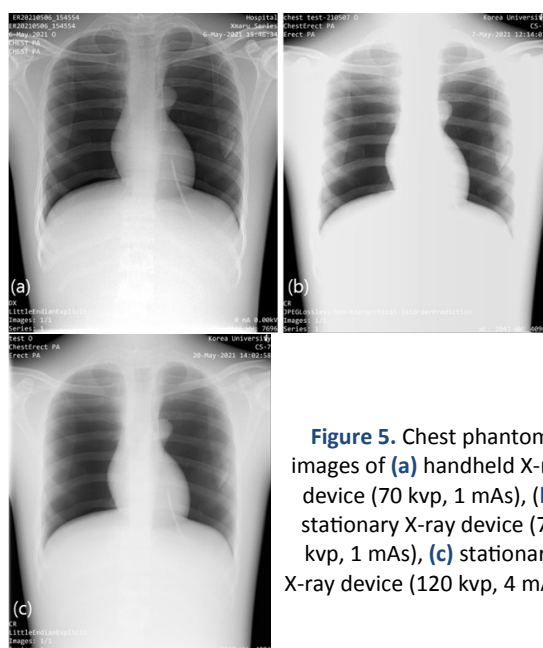


**Figure 5.** Chest phantom images of (a) handheld X-ray device (70 kVp, 1 mAs), (b) stationary X-ray device (70 kVp, 1 mAs), (c) stationary X-ray device (120 kVp, 4 mAs).



**Figure 6.** Comparison of phantom radiography images.

Radiography images of handheld X-ray device (a-1) skull phantom radiograph, (a-2) knee phantom radiograph, (a-3) elbow phantom radiograph, (a-4) hand phantom radiograph;

Radiography images of stationary X-ray device: (b-1) skull phantom radiograph, (b-2) knee phantom radiograph, (b-3) elbow phantom radiograph, (b-4) hand phantom radiograph.

## DISCUSSION

Currently, more than 95% of HXDs are used in dental imaging, however, their application is expanding to other major medical fields. In clinical practice, performing chest radiography with an HXD has several advantages. These devices are, on average, 100 times lighter than SXDs, and often use a lithium-ion battery, which has high efficiency. Furthermore, HXDs can easily be used in various places with a single charge, including outside the hospital environment, and are generally less expensive than SXDs<sup>(30)</sup>.

In line with this global trend, the accuracy of the tube voltage, reproducibility of the X-ray dose, linearity, leakage dose, accuracy of the focal spot size, and phantom images were analyzed to evaluate the diagnostic image quality. The accuracy of the tube voltage and the reproducibility and linearity of the X-ray dose were measured to reduce the frequency of patient reimaging as a performance evaluation of the devices. Both the HXD and SXD experiments were conducted under the same conditions, and the results were compared to evaluate their performances. The PAE value of the tube voltage was -0.01% for HXD, and the error of the tube voltage was 0.01% for SXD, which is lower than the standard of 10%. According to the International Electrotechnical Commission (IEC) 60601-2-54 standard, the PAE of the tube voltage must be within  $\pm 10\%$  of the set value; therefore, both devices showed accurate tube voltages<sup>(31)</sup>.

Furthermore, the reproducibility and linearity of the radiation dose were used to evaluate the performance and reliability of the devices, and the average CV of the radiation dose emitted under the same conditions was 0.002 for the HXD. According to the IEC 60601-2-54 standard, the reproducibility of the radiation dose evaluates the performance and reliability of an X-ray device. Therefore, the CV of the X-ray dose emitted under the same conditions should be less than 0.05<sup>(31)</sup>.

Evaluating secondary radiation to radiologic technologists or other medical staff is very important, especially in emergencies where radiologic technologists cannot stand behind the radiation shielding partition and must hold the HXD to complete the radiography procedure, such as when mounting the HXD on a tripod is not feasible.

According to the recommendations of the National Council on Radiation Protection and Measurements Report (NCRP) No. 10, when a diagnostic radiation generator is used outside a medical institution in an area where a mobile radiography transport bus cannot travel, a radiation shielding partition must be installed. The leakage dose measured from behind the partition should be less than 1 mSv/year<sup>(32-33)</sup>. All six sides of the HXD

were measured, and the leakage doses from the right and left sides were 5 times more than those from the rear side. One study focusing on the dental use of an HXD evaluated the radiation dose and found that a 2–3 times higher dose was exposed near 140° and 220° of the handles <sup>(34)</sup>. Another study evaluated the leakage dose using a dental HXD, with the highest dose in the vicinity of the left palm, and found that the average exposure was 0.031 mSv <sup>(35)</sup>. Radiological technologists should physically be behind these devices rather than on the side to avoid exposure to leaked doses when performing imaging. In addition, assuming even the highest leakage dose when using an HXD according to these standards, medical staff is considered safe from exposure to leakage dose because the leakage dose is 0.26 mSv/year without the use of a partition.

In general, if an image is enlarged for image evaluation, the intrinsic resolution of the detector improves; however, the overall resolution is lowered because the effect of blurring according to the size of the focal spot is large. The accuracy of the focal spot size was measured to determine the resolution of the images. It should be constructed so that all straight-line intersection areas of the X-ray device pass through the radiation aperture of the device. According to the IEC 60601-2-54 standard, the measured focal spot size must have an error rate within  $\pm 50\%$  of the nominal focal spot size provided by the device manufacturer <sup>(31)</sup>. In this experiment, the average of the long-axis direction and the vertical direction of the HXD was 49%, which had an error rate of less than 50%. Because the HXD pixel size of the image receptor is 127  $\mu\text{m}$ , when the beam is aligned correctly, the focal spot point in the long-axis direction of the X-ray tube forms on four horizontally parallel pixels (0.508 mm). Therefore, considering the pixel size of the image receptor, the error rate of the focal size in the long-axis direction of the X-ray tube was 22%, which matches the nominal focal size.

Finally, to compare the image quality, including resolution and contrast, five types of phantoms were photographed under the same exposure conditions in both devices. Two images taken using 70 kV and 2 mAs through chest phantom imaging were compared, and the resolution of the images taken with the HXD was found to be clearer, as were the pulmonary blood vessels, diaphragm, thoracic intervertebral disc, and bronchial tubes of the entire lung field. In addition, capturing images using 120 kV and 4 mAs, which are the existing imaging conditions of an SXD, resulted in a resolution and sharpness similar to those of an SXD. Therefore, when the HXD was used with a small dose, it was possible to obtain an image with a resolution and clarity similar to that of existing X-ray imaging.

Although various performance evaluations have been conducted, there are some limitations. First, because only one type of HXD was analyzed, it was difficult to generalize the findings to other HXDs.

Second, the image quality results were derived using phantoms, as opposed to patients in a clinic. However, this study was conducted to reduce the disadvantages of the current medical market and to evaluate the suitability of HXD in a pandemic situation.

## CONCLUSION

This study evaluated the performance of an HXD in contrast with an SXD to determine whether HXDs are suitable for use during a pandemic and to ensure that proper image quality can be obtained both inside and outside a hospital. The accuracy of the tube voltage, reproducibility of the X-ray dose, linearity, leakage dose, accuracy of the focal spot size, and quality of the phantom images were obtained and compared. The value for diagnosis was optimal, and it was concluded that the leakage radiation dose would be safe at 0.26 mSv/year without using a radiation shielding partition. Ultimately, it was found that images of appropriate quality can be obtained with an HXD without causing significant exposure to medical staff, the general public, or patients outside hospitals.

## ACKNOWLEDGMENT

This research was supported by the Promotion of Innovative Businesses for Regulation-Free Special Zones, funded by the Ministry of SMEs and Startups (MSS, Korea) (P0011221).

**Ethics approval and consent to participate:** Not applicable.

**Conflict of Interest:** The authors declare no conflict of interest.

**Funding:** Not applicable.

**Authors' contributions:** All authors contributed equally to the design of the study, data collection and analysis, and writing of the manuscript. All authors have read and approved the final manuscript.

## REFERENCES

1. Benmalek E, Elmhamdi J, Jilbab A (2021) Comparing CT scan and chest X-ray imaging for COVID-19 diagnosis. *Biomed Eng Adv*, **1**: 1-6.
2. Kim EH, Choi YS, Park HM, Na CY, Kim JM, Kim JS, Han TH (2021) Assessment of radiation dose of mobile computed tomography in intensive care units. *Radiat Prot Dosim*, **196** (1-2): 60-70.
3. Venkateshgowda P, Rao S, Mutkule D, Taggu A (2014) Unexpected events occurring during the intra-hospital transport of critically ill ICU patients. *Indian J Crit Care Med*, **18** (6): 354-7.
4. Parmer H, Lim TC, Goh J, Tan J, Sitoh Y, Hui F (2004) Providing optimal radiology service in the severe acute respiratory syndrome outbreak: use of mobile CT. *Am J Roentgenol*, **58**: 57-60.
5. Waydhas C, Schneck G, Duswald KH (1995) Deterioration of respiratory function after intra-hospital transport in critically ill surgical patients. *Intensive Care Med*, **21**: 784-789.
6. Waydhas C (1999) Intra hospital transport of critically ill patients. *Crit. Care.*, **3**(5): R83-R89.
7. Yoon SH, Lee KH, Kim JY, et al. (2020) Chest radiographic and CT

- findings of the 2019 novel coronavirus disease (COVID-19): analysis of nine patients treated in Korea. *Korean J Radiol*, **21(4)**: 494-500.
8. Xie X, Zhong Z, Zhao W, Zheng C, Wang F, Liu J (2020) Chest CT for typical 2019-nCoV pneumonia: relationship to negative RT-PCR testing. *Radiology*, **296(2)**: E41-45.
  9. Leonardi A, Scipione R, Alfieri G et al. (2020) Role of computed tomography in predicting critical disease in patients with covid-19 pneumonia: A retrospective study using a semiautomatic quantitative method. *Eur J Radiol*, **130**: 1-7.
  10. Peace K, Wilensky EM, Frangos S, et al. (2010) The use of a portable head CT scanner in the intensive care unit. *J Neurosci Nurs*, **42(2)**: 109-116.
  11. Gance CP, Pahade JK, Gortopassi I, et al. (2020). Social distancing with portable chest radiographs during the COVID-19 pandemic: assessment of radiograph technique and image quality obtained at 6 feet and through glass. *Radiology*, **2(6)**: 1-7.
  12. Sawicka BD (1995), Portable digital electronic radiography system. *Candu Maintenance Conference, Ontario, Canada*, 71-77.
  13. Jacobi A, Chung M, Bernheim A, Eber C (2020) Portable chest X-ray in coronavirus disease-19 (COVID-19): A pictorial review. *Clin Imaging*, **64**: 35-42.
  14. Eisenhauber E, Schaefer-Prokop CM, Prosch H, Schima W (2012) Bedside chest radiography. *Respir Care*, **57(3)**: 427-443.
  15. Cohen MD, Long B, Cory DA, Broderick NJ, Smith JA (1989) Digital imaging of the newborn chest. *Clin Radiol*, **40**: 365-368.
  16. Hong DH, Lim CH, Kim YM, et al. (2021) Necessity of mandatory records on radiological examination. *J Radiol Sci Technol*, **44(4)**: 399-407.
  17. Choi PK (2021) Quality control of diagnostic X-ray equipment in medical field. *J Korean Soc Radiol*, **15(2)**: 159-64.
  18. Kastan DJ, Ackerman LV, Feczko PJ, Beute GD (1985) Digital radiograph: a review. *Henry Ford Hosp Med J*, **33(2-3)**: 88-94.
  19. Smathers RL and Brody WR (1985) Digital radiograph: current and future trends. *Br J Radiol Suppl*, **58**: 285-307.
  20. Korner M, Weber CH, Wirth S, Pfeifer K, Reiser MF, Treitl M (2007) Advances in digital radiography: physical principles and system overview. *Radiographics*, **27**: 675-686.
  21. Jennings P, Padley SP, Hansell DM (1992) Portable chest radiography in intensive care: a comparison of computed and conventional radiography. *Br J Radiol*, **65**: 852-856.
  22. Kim TH, Heo DW, Jeong CW, Ryu JH, Hong YJ, Han SJ, Han TU, Yoon KH (2017) Development of portable digital radiography system with a device for monitoring X-ray source-detector angle and its application in chest imaging. *Sensors*, **17**: 531.
  23. Van Dis ML, Miles DA, Parks ET, Razmus TF (1993) Information yield from a hand-held dental x-ray unit. *Oral Surg Oral Med Oral Pathol*, **76**: 381-385.
  24. Kumar GA, Kumar RP, Malleswararao V (2011) Evaluation on X-ray exposure parameters considering tube voltage and exposure time. *Int J Eng Sci Technol*, **3(4)**: 3210-3215.
  25. Rolf B (2021) Modern diagnostic X-ray sources: Technology, Manufacturing, Reliability. 2<sup>nd</sup> ed., CRC Press, Florida.
  26. Kase KR, Svensson GK, Wolbarst AB, Marks Ma (1983) Measurements of dose from secondary radiation outside a treatment field. *Int J Radiation Oncology Biol Phys*, **9(8)**: 1177-1183.
  27. The National Academics (2006) Health risks from exposure to low levels of ionizing radiation: BEIR VII Phase 2. Board on Radiation Effects Research. National Research Council of the National Academies. Washington, D.C.
  28. Chaney EL and Hendee WR (1974) Effects of X-ray tube current and voltage on effective focal-spot size. *J Med Phys*, **1(3)**: 141-147.
  29. Mocy SF and Shazli ZA (2018) A phantom study for the optimization of image quality and radiation dose for common radiography examinations in digital radiography. *Iran J Med Phys*, **15(4)**: 271-276.
  30. Seilern-Moy K, Vielgrader H, Gerritsmann H, Walzer C (2018) Radiography in the field: assessing a lightweight, handheld, battery-powered dentistry unit for field diagnostic applications. *J Zoo Wildl Med*, **48(1)**: 31-39.
  31. International Electrotechnical Commission (2009) IEC 60601-2-54: 2009 Medical electrical equipment- Part 2-54: particular requirements for the basic safety and essential performance of X-ray equipment for radiography and radioscopy.
  32. National Council on Radiation Protection and Measurements (2004) Recent applications of the NCRP public dose limit recommendation for ionizing radiation: NCRP Report 10. (Maryland, United States of America: National Council on Radiation Protection and Measurements (NCRP).
  33. National Council on Radiation Protection and Measurements (2005) Structural shielding design for medical X-ray imaging facilities: NCRP Report 147. (Maryland, United States of America: National Council on Radiation Protection and Measurements (NCRP).
  34. Rottke D, Gohlke L, Schrodel R, Hassfeld S, Schulze D (2018) Operator safety during the acquisition of intraoral images with a handheld and portable X-ray device. *Dentomaxillofac Radiol*, **47**: 1-9.
  35. Makdissi J, Pawar RR, Johnson B, Chong BS (2016) The effects of device position on the operator's radiation dose when using a handheld portable X-ray device. *Dentomaxillofac Radiol*, **45**: 1-7.

